Probing Solvent Polarity across Strongly Associating Solid/Liquid Interfaces Using Molecular Rulers

X. Zhang,[†] W. H. Steel,[‡] and R. A. Walker*[,†,‡]

Department of Chemistry and Biochemistry, University of Maryland, College Park, College Park, Maryland 20742

Received: September 12, 2002; In Final Form: December 30, 2002

A new family of neutral, solvatochromic surfactants has been used to probe solvent polarity across strongly associating solid/liquid interfaces. The surfactants consist of *p*-nitroanisole-based chromophores and polar −OH groups separated by alkyl chains of different lengths. The solid substrate is silanol-terminated, hydrophilic silica, and the strongly associating solvents are 1-butanol and 1-octanol. To understand how the chromophore itself interacts with the hydrophilic substrate, we acquire resonance enhanced second harmonic (SH) spectra of the bare chromophore adsorbed to the silica/cyclohexane, solid/liquid interface. Spectra show two features despite the chromophore having only a single electronic resonance in the wavelength region (∼300 nm) examined. These features are assigned to the chromophore adsorbed to the surface in two different orientations. Second harmonic spectra of the bare chromophore adsorbed to the hydrophilic/butanol and hydrophilic/octanol interfaces again show two features with the less polar, shorter wavelength feature being more pronounced in the octanol spectrum. Despite exhibiting pNAs-like behavior in bulk solution, molecular rulers present a very different picture of interfacial polarity. SH spectra from the hydrophilic/butanol interface indicate that interfacial polarity is enhanced over bulk solution limits. Furthermore, spectra lose their bimodal appearance, indicating that local polarity is rather uniform across the interfacial region. In contrast, the hydrophilic/octanol interface continues to show bimodal behavior for all of the molecular rulers studied, suggesting that surface-induced changes in solvent structure partitions solvent polarity into regions that are more polar and less polar than bulk solution. Data from the hydrophilic/octanol system suggest that variations in solvent polarity extend no more than ∼1.2 nm into solution or approximately the length of a fully extended, 1-octanol molecule.

1. Introduction

Solid/liquid interfaces figure prominently in a host of chemical phenomena ranging from chromatographic retention[1,2] to crystallization[3] to protein recognition at membrane surfaces.[4] Intuition tells us that the properties of solid/liquid interfaces depend sensitively on the identity of both the substrate and the adjacent solvent, but despite their fundamental and technological importance, solid/liquid interfaces have evaded the rigorous, quantitative inquiries that have characterized gas/liquid and gas/solid boundaries.[5] Experimentally, interfaces between two condensed phases—or "buried interfaces"—are difficult to probe noninvasively. Furthermore, modeling buried interfaces requires making severe approximations in order to solve extensive many-body interactions.[6−9] Thus, even though "common sense" may guide our understanding of solid/liquid interfacial behavior, many fundamental questions about these systems remain unanswered. In the experiments described below, we attempt to address one such question: "How far into solution do interfacial effects extend?" Specifically, experiments probe solvent polarity across strongly associating solid/liquid interfaces using newly created, solvatochromic surfactants and surface-specific, resonance-enhanced second harmonic (SH) generation. Results support recent observations that dielectric properties can partition at the boundaries between strongly interacting solids and liquids.[10−12] These interfacial regions have properties that do not scale with surface or bulk solvent properties. Furthermore, findings imply that variations of solvent polarity within these strongly associating systems extend ∼1 solvent length away from the hydrophilic solid surface.

Traditionally, two different optical methods have been used to probe solvation at buried interfaces: NLO spectroscopy[13] and fluorescence in a total internal reflection (TIR) geometry.[14] Here, the term solvation describes noncovalent interactions experienced between a solute and its surroundings. TIR fluorescence is a linear spectroscopy meaning that results are often much simpler to interpret than spectral data from NLO experiments. However, unlike second-order NLO spectroscopy, selection rules do not constrain the fluorescence response to only the interfacial region. Even in a TIR geometry, the evanescent excitation field penetrates tens of nanometers into bulk solution. Consequently, TIR fluorescence can arise from solutes in a variety of environments ranging from extremely inhomogeneous to isotropic. Not surprisingly, the two different methods often lead to competing descriptions of how surfaces affect interfacial solvation.[11,12,15−34]

Optical experiments probing surface polarity, solvent relaxation, and solute activities necessarily probe gradients across an interfacial region. Uncertainty in the spatial extent of these gradients can cloud the interpretation of results. Both neutron and X-ray scattering methods *can* measure density and concentration gradients quantitatively,[35−40] but these techniques are unable to discern noncovalent, intermolecular interactions responsible for chemical solvation. Molecular simulations can identify how a chemical environment changes across interfacial regions and describe quantitatively gradients in solvation properties near a surface.[41−48] Michael and Benjamin illustrated this capability by calculating solvent relaxation response func-

[†] Chemical Physics Program, University of Maryland, College Park.
[‡] Department of Chemistry and Biochemistry University of Maryland, College Park.

10.1021/jp022067+ CCC: $25.00
Published on Web 03/29/2003

tions around a model chromophore placed different distances away from a sharp, liquid/liquid interface.[49] The authors predicted that changing probe−surface separation by as little as 5 Å led to a *2 orders of magnitude* change in solvent relaxation rates. Such findings motivate the need to examine interfacial properties across *molecular* length scales.

The work presented below adopts the spirit of these (and other) simulations of solvation at buried interfaces. Ideally, when profiling solvation across an interfacial region, one would like to vary the solute distribution such that one set of experiments probes the interfacial chemical environment ~1 solvent diameter away from the surface and a second set of experiments probes the environment at 2 solvent diameters, etc. We attempt to address this issue by using molecular rulers of varying lengths adsorbed to strongly associating hydrophilic/1-butanol and hydrophilic/1-octanol solid/liquid interfaces. Hydrophilic surfaces correspond to silanol-terminated fused silica. Molecular rulers refer to a series of newly created solvatochromic surfactants consisting of a hydrophobic, solvent-sensitive chromophore attached to a polar headgroup by means of variable length alkyl spacers.[50] The polar headgroup can interact strongly with the polar substrate, enabling the chromophore to "float" into the adjacent solvent. Measuring how the solvent sensitive response of the chromophore varies with probe/headgroup separation enables experiments to profile variations in solvent polarity across the interfacial region.

In the remainder of this paper, we first describe experimental considerations including the creation of molecular ruler surfactants. To interpret the second harmonic spectra of molecular rulers, we first examine the behavior of the parent chromophores at both weakly and strongly associating interfaces. We then vary the equilibrium distribution of solutes across the interface by recording resonance-enhanced second harmonic spectra of different length molecular rulers adsorbed to these same boundaries. Spectra show that the hydrophilic/1-butanol system presents an interfacial environment that is considerably more polar than bulk solution and does not vary significantly over the 0.5−1.5 nm spanned by different length rulers. In contrast, the hydrophilic/1-octanol system partitions into two distinct regions, and the nonpolar region extends approximately the length of a fully extended 1-octanol molecule.

2. Experimental Considerations

2A. Solvatochromism as a Probe of Interfacial Polarity. Solvatochromism refers to a solute's solvent-sensitive, electronic transition energy.[51,52] When a gas-phase chromophore becomes solvated, its eigenstate energies are lowered by noncovalent interactions with the solvent medium. The resulting difference in transition energies represents the chromophore's solvation energy. If the chromophore's excited-state dipole is larger than its ground-state dipole, the excited state will be preferentially solvated, leading to a spectroscopically observable red shift in the solute excitation spectrum (Figure 1a). This red shift becomes more pronounced with increasing solvent polarity. Thus, solvatochromic behavior can serve as a sensitive measure of solvation by probing local solvent properties. Solutes that are sensitive to long-range forces arising from solvent permittivity generally exhibit monotonic solvatochromic behavior as a function of solvent polarity[52] (Figure 1b). Solvent polarity is characterized in terms of the Onsager polarity function,[53] $f(D)$, where

$$f(D) = \frac{2(D-1)}{2D+1} \qquad (1)$$

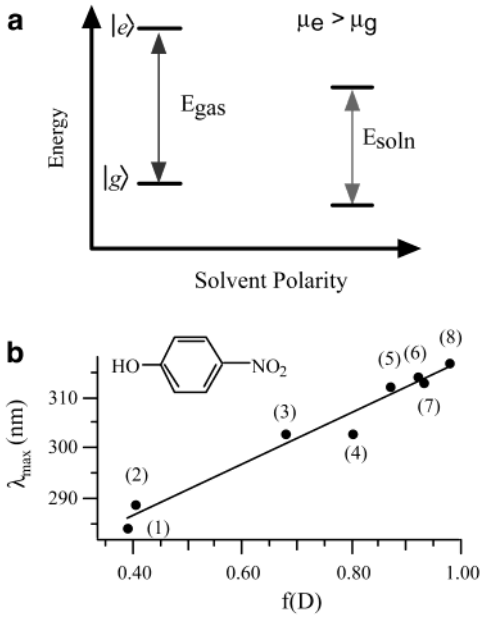

Figure 1. (a) Schematic diagram describing origins of solvatochromic effect. (b) Solvatochromic behavior of *p*-nitrophenol in various solvents. Points correspond to excitation maxima. Spectra were recorded with a HP 8452A diode array spectrophotometer. Solute concentrations were adjusted to keep maximum absorbance below 1.0 OD. Solvents correspond to (1) isooctane, (2) cyclohexane,(3) ethyl ether, (4) ethyl acetate, (5) 1-butanol, (6) ethanol, (7) acetonitrile, and (8) water.

TABLE 1: Excitation Maxima (in nm) of *p*-Nitrophenol (pNP), *p*-Nitroanisole (pNAs), C_2 Ruler, and C_5 Ruler in Various Solvents[a]

solvent/solute	pNP	pNAs	C_2 ruler	C_5 ruler
isooctane	286	292	292	295
cyclohexane	288	294	293	297
ethyl ether	303	300	302	302
1-octanol	312	303	304	306
1-butanol	314	303	306	308
acetonitrile	314	305	310	312
water	318	316	317	319

[a] Data were acquired according to procedures described in text. Excitation spectra were fit to single, Gaussian feature and showed no evidence of asymmetric broadening. Aqueous pH was 6.2 for all spectra acquired in water.

and D is a solvent's static dielectric constant. Given their small sizes, photochemical stability, and pronounced solvatochromic behavior, *p*-nitrophenol (pNP) and its alkylated derivative, *p*-nitroanisole (pNAs), stand out as ideal chromophores for probing solvent polarity across solid/liquid interfaces. Excitation maxima of all solutes in various bulk solvents are presented in Table 1.

2B. Probes of Solvent Polarity across Solid/Liquid Interfaces: Molecular Rulers. Profiling chemical properties across interfacial regions requires systematically varying the equilibrium distribution of probes relative to the solid/liquid boundary. We accomplish this goal by joining a *p*-nitroanisole-based chromophore to a *n*-alcohol alkyl chain via the following procedure:[50]

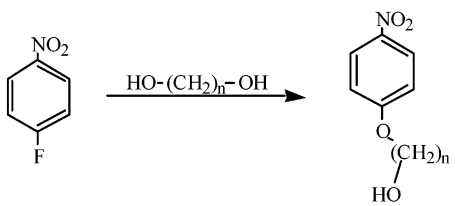

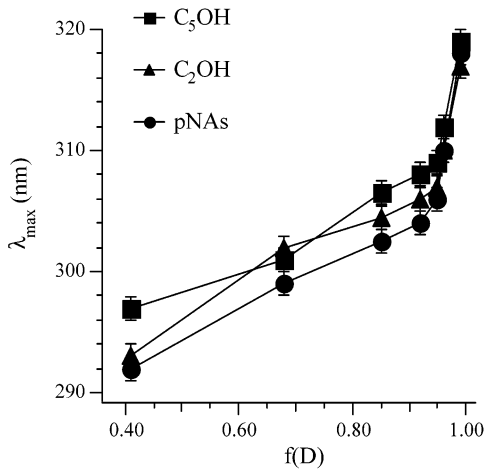

Figure 2. Solvatochromic behavior of *p*-nitroanisole and the C_2 and C_5 molecular rulers in various solvents. Points correspond to excitation maxima. Spectra were recorded with a HP 8452A diode array spectrophotometer. Solute concentrations were adjusted to keep maximum absorbance below 1.0 OD. Solvents (from left to right): cyclohexane, ethyl ether, 1-octanol, 1-butanol, ethanol, acetonitrile, and water.

In this work, we refer to the chromophore−alcohol chain assembly as a molecular ruler.[50] The term C_n ruler refers to molecular rulers having *n* methylene groups in the alkyl chain. Figure 2 shows that attaching alkyl chains of varying lengths to the aromatic chromophore does not significantly alter the chromophore's solvatochromic activity. In bulk solution the pNAs excitation maxima range from 292 nm (cyclohexane) to 316 nm (water). Excitation maxima of the molecular rulers are consistently red-shifted by ∼2 nm from the pNAs values, but the overall behavior is unchanged. Given a limiting resolution of ±2 nm in most SH spectra, we treat C_2 and C_5 solvatochromic data in Figure 2 as being equivalent to that of pNAs. pNAs is approximately 20 times more soluble in nonpolar solvents (e.g., cyclohexane) than in water,[50] meaning that, given the opportunity, the aromatic chromophore in molecular rulers should interact preferentially with the organic solvent. The −OH functional group can hydrogen bond to the hydrophilic surface. In the spectra presented below, we observe that the solvatochromic probes sample a variety of environments across the interfacial region, some of which can be assigned to the surfactant −OH interacting directly with the surface.

The excitation probed by SH experiments corresponds to a $\pi-\pi^*$ transition that can be represented as a partial charge transfer between the ether oxygen and the nitro group in the para position. This transition forms the basis of the empirical π^* solvent polarity scale,[53] and the $\Delta\mu$ of +8 D[54] accounts for the strong dependence of excitation wavelengths on solvent polarity. An important point to emphasize is that in bulk solution this $\pi-\pi^*$ excitation is the only transition with appreciable intensity in the 300 nm region. Data described below will show that at interfaces the pNAs-based probes sometimes show evidence of two electronic transitions, implying that chromophores sample two distinctly different dielectric environments across the interfacial region.

2C. Probing Interfacial Solvatochromism: Resonance-Enhanced Second Harmonic Generation. Second harmonic generation (SHG) is a nonlinear optical method that can measure effective excitation spectra of species at interfaces.[12,13,25,55] Because of its origins, SHG is both surface and molecularly specific, meaning that spectra result only from solutes that experience interfacial anisotropy. In a typical SHG experiment, a single coherent optical field with frequency ω is focused on the interface under study, and a nonlinear polarization with frequency 2ω is detected. The intensity of the 2ω field is proportional to the square of the second-order susceptibility, $\chi^{(2)}$[56]

$$I(2\omega) \propto |\chi^{(2)}|^2 I^2(\omega) \tag{2}$$

where $I(\omega)$ is the intensity of the incident field and $\chi^{(2)}$ is a third rank tensor that under the electric dipole approximation is zero in isotropic environments. The $\chi^{(2)}$ tensor is responsible for the technique's inherent surface specificity and contains both nonresonant and resonant contributions:

$$\chi^{(2)} = \chi^{(2)}_{NR} + \chi^{(2)}_{R} \tag{3}$$

For dielectric systems the resonant term is typically several orders of magnitude larger than the nonresonant contribution and can be related to microscopic hyperpolarizability:[57]

$$\chi^{(2)}_{R} = N\sum_{k,e} \frac{\langle A_{k,e}\rangle}{(\omega_{gk} - \omega - i\Gamma)(\omega_{eg} - 2\omega + i\Gamma)} \tag{4}$$

where the sum extends over all (virtual) intermediate and excited states, *k* and *e*, respectively. *N* corresponds to the number of molecules being probed, $\langle A_{k,e}\rangle$ is the orientationally averaged molecular hyperpolarizability, the ω_{ij} refer to transition energies between the ground state and states *k* and *e*, and Γ is a transition's line width. When 2ω is resonant with ω_{eg}, $\chi^{(2)}$ becomes large, leading to a strong resonance enhancement in the observed intensity at 2ω. Thus, measuring the scaled intensity $[I(2\omega)/I^2(\omega)]$ as a function of 2ω records an *effective* excitation spectrum of solutes adsorbed to an interface. SH spectra reported in this work were all acquired under $P_\omega P_{2\omega}$ polarization conditions. Spectra acquired with alternative polarizations showed no significant differences from the $P_\omega P_{2\omega}$ data.

Data presented below motivate the need to fit some spectra to two resonance features despite the fact that, in bulk solution, there exists only one electronic transition ∼300 nm. We will propose that the two features arise from two different chromophore orientations. Two orientations lead to the chromophores sampling two different local environments and, consequently, having two different electronic excitation energies. Accounting for a second resonance requires expanding the summation in eq 4 to include two resonance terms, and eq 3 becomes

$$\chi^{(2)} = \chi^{(2)}_{a} + \chi^{(2)}_{b} + \chi^{(2)}_{NR} \tag{5}$$

where $\chi^{(2)}_a$ and $\chi^{(2)}_b$ correspond to the resonance-enhanced contributions from the two spectral features, a and b. Analysis of spectra presented below will focus on four quantities: the two excitation maxima (λ_a and λ_b (from ω_{ag} and ω_{bg})) and the line strength terms A_a and A_b corresponding to the two bands. Line widths (Γ_a and Γ_b) vary very little. The nonresonant term, $\chi^{(2)}_{NR}$, is small but does lead to differences between the calculated excitation maxima and the apparent spectral maxima. When fitting a spectrum, the relative magnitudes of the two linestrength terms are monitored closely. If $A_a/A_b > 5$, the second feature is deemed inconsequential with respect to the observed SH intensity, and the spectrum is refit with only a single resonance term. This situation arises exclusively for the hydrophilic/1-butanol solid/liquid systems.

2D. Specific Experimental Considerations. All solutions have solute concentrations between 0.5 and 2 mM. These

concentrations lead to surface coverages of less than 15% of a full monolayer according to adsorption isotherms recorded with different alcohol solvents. To within experimental error, 2-fold changes in bulk solution concentration do not alter spectral profiles of adsorbed rulers, indicating that solute−solute interactions at the surface do not perturb interfacial solvent polarity. Solid/liquid interfaces are created by placing a fused silica prism (Edmund Industrial Optics) hypotenuse side down onto a Teflon cell containing a reservoir of solution. Prior to use, prisms are cleaned in a 50:50 mixture (by volume) of concentrated sulfuric and fuming nitric acid. Clean prisms always exhibited complete wetting by an aqueous solvent. According to previous studies, these surfaces should have surface silanol concentrations of $\sim 5 \times 10^{14}/\text{cm}^2$.[58]

The SHG apparatus is built around a Ti:sapphire regeneratively amplified, femtosecond laser (Clark-MXR CPA2001) that produces 130 fs pulses with energies of $\sim 700\ \mu$J at a wavelength of 775 nm and repetition rate at 1 kHz. The output of the Ti:sapphire laser pumps a commercial optical parametric amplifier (OPA, Clark-MXR). The visible output of the OPA is tunable from 560 to 700 nm, with the bandwidth of 2.5 ± 0.5 nm. The polarization of the incident beam is controlled using a Glan-Taylor polarizer and a half-wave plate. A series of filters block the fundamental 775 nm and any second harmonic light generated from the preceding optical components. Second harmonic photons are detected in the reflected direction using photon counting electronics. Typical signal levels average 0.01−0.1 photon per shot. A second polarizer selects the polarization of the SH signal. A short pass filter and monochromator serve to separate the second harmonic signal from background radiation.

Because the visible OPA cannot be synchronously tuned, acquisition of a complete SHG spectrum requires multiple hours. A typical procedure entails letting the solid/liquid system equilibrate (as evidenced by an unchanging SH intensity), followed by manual tuning of ω_{vis} to each desired wavelength. System alignment is reoptimized at every wavelength to account for the wavelength-dependent refractive indices of the prism and collection optics. At each wavelength, SH data are collected for three 10 s intervals and normalized for incident power. Although tedious, this procedure ensures that spectra are reproducible. A single wavelength might be sampled three separate times several hours apart (beginning, middle, and end of acquisition sequence). If the normalized SH signal from each of these three samples does not fall within the limits of experimental uncertainty, data acquisition is halted and the spectrum discarded. In addition, data at the same wavelength were often acquired using several different incident powers and then normalized to confirm the quadratic dependence of SH signal intensity on the incident field intensity predicted by eq 2. Predicted quadratic behavior was always observed.

3. Results and Discussion

3A. pNAs and pNP at Weakly Associating Interfaces. The first goal of this work is to identify how the ruler chromophore interacts with a hydrophilic, silica substrate. Figure 3 shows the SH spectrum of pNAs adsorbed to the weakly associating, hydrophilic, silica/cyclohexane interface. Shown for comparison is the SH spectrum of *p*-nitrophenol (pNP) adsorbed to the same interface. Two features are apparent in both spectra. In the pNAs system, the longer wavelength feature at 328 nm carries significant intensity with a second, weak feature appearing at 295 nm. The relative intensities of the two features in the pNP spectrum are reversed: the shorter wavelength feature (300 nm) shows higher intensity than the longer wavelength feature (321 nm). (Optimized fitting parameters are listed in Table 2.)

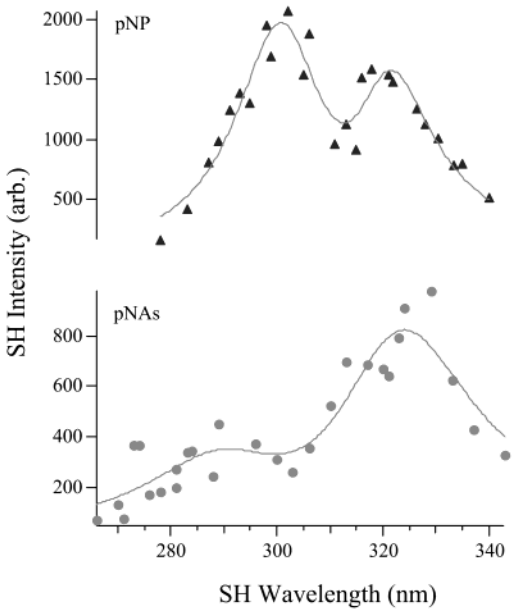

Figure 3. SH spectra of pNAs (lower panel) and pNP (upper panel) adsorbed to the hydrophilic/cyclohexane interface. Solid lines represent fits to the experimental data according to eqs 2−5. Fit parameters appear in Table 2.

TABLE 2: Optimized Parameters from Fitting Data Shown in Figures 3 and 5−7 to Equations 2−5[a]

solute	solvent	λ_a (nm)	A_a ($\times 10^3$)	λ_b (nm)	A_b ($\times 10^3$)
pNAs	cyclohexane	295 ± 3	0.5	328 ± 2	3.8
pNP	cyclohexane	302 ± 1	3.9	321 ± 1	2.7
pNAs	1-butanol	304 ± 2	0.8	321 ± 2	1.5
pNAs	1-octanol	307 ± 3	4.0	324 ± 2	1.5
C_2 ruler	1-butanol	316 ± 3	7	NA	NA
C_2 ruler	1-octanol	296 ± 2	3.8	316 ± 2	11.4
C_4 ruler	1-butanol	326 ± 2	1.6	NA	NA
C_4 ruler	1-octanol	309 ± 1	2.8	325 ± 2	1.5
C_5 ruler	1-butanol	324 ± 2	7.0	NA	NA
C_5 ruler	1-octanol	305 ± 2	3.6	321 ± 1	2.7

[a] Line widths typically ranged from 25 to 40 nm fwhm, and the nonresonant contribution to the SH spectrum never exceeds 5% of the resonant contribution. Additional details about fitting spectra are describe in the text.

This behavior is puzzling because in bulk solution both chromophores show only a single electronic excitation in the 300 nm region. Assuming a single electronic transition, the SH spectra in Figure 3 suggest that the solutes experience two distinctly different environments at the hydrophilic/cyclohexane solid/liquid interface: one that is polar (corresponding to the long wavelength feature) and one that is less polar (corresponding to the short wavelength feature). The only significant difference between pNP and pNAs is the identity of the functional group para to the nitro group. The alcohol moiety on pNP enables this solute to act as a hydrogen-bond donor (through the −OH) as well as a hydrogen-bond acceptor (primarily through the $-NO_2$). pNAs can only accept hydrogen bonds.

Given two solute/substrate interaction mechanisms for pNP (H-bond donor and acceptor), assigning the two features in the pNP spectrum to "$-NO_2$ up" (pNP as H-bond donor) and "$-NO_2$ down" (pNP as H-bond acceptor) orientations is reasonable. There remains the challenge of correlating each orientation with its respective feature in the pNP spectrum. Bulk solution, solvatochromic studies of pNP show that strengthening solvent−solute interactions leads to increasingly red-shifted excitation wavelengths[24] (Figure 1). Thus, the task of assigning

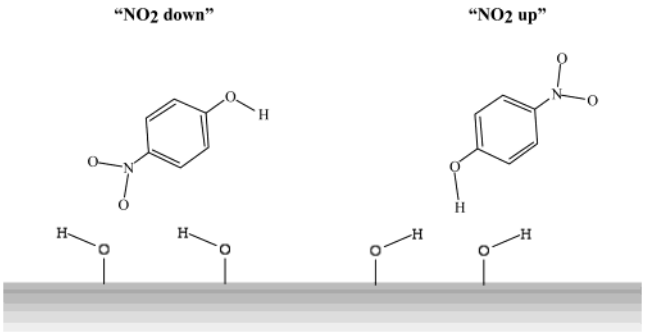

Figure 4. Illustration of two different possible orientations of pNP at a hydrophilic solid substrate. The NO_2 down orientation leads to a pronounced red shift in the chromophore excitation wavelength due to strong NO_2−substrate interactions. In contrast, the NO_2 up orientation allows the chromophore to interact with the interfacial solvent species. The basis for these assignments is described in the text. Both orientations are shown with the long axis of the molecule deflected ∼50° away from surface normal in accord with polarization-dependent SH intensity measurements.

the two pNP spectral features reduces to determining which orientation will lead to stronger interactions between the solute and its environment. Generally speaking, a nitro group possesses a dipole moment (3−4 D depending on the molecule) that is twice as large as that of a hydroxyl group (1.5−2 D).[59] Consequently, we expect stronger interactions between the pNP $-NO_2$ group and the polar, hydrophilic substrate than between the pNP −OH group and the surface. This reasoning assigns the long wavelength feature (at 321 nm) in the pNP spectrum to the "$-NO_2$ down" configuration and the short wavelength feature (at 300 nm) to the "$-NO_2$ up" orientation. Given equivalent molecular orientations calculated from polarization-dependent SH intensities (vide infra), the comparable intensities associated with the short and long wavelength features suggest comparable populations of both orientations.

These assignments are supported by the SH spectrum of pNAs adsorbed to the cyclohexane/hydrophilic liquid/solid interface. The methoxy group of pNAs prevents this solute from functioning as a hydrogen-bond donor. In principle, both the $-NO_2$ and the ether oxygen can accept hydrogen bonds from the surface, but given the large disparity in dipole magnitude (3−4 D for the $-NO_2$ group, 1−1.3 D centered on the ether oxygen), we expect solute−surface interactions through the nitro group to control interfacial solute concentration and orientation. The SH spectrum of pNAs adsorbed to the hydrophilic surface shows a strong, pronounced feature centered at 328 nm and a much weaker feature at 295 nm. This pattern is consistent with a pNAs solute that interacts strongly with the surface through the polar $-NO_2$ group (leading to a pronounced red shift in the spectrum and a large integrated intensity) but only weakly through the ether linkage (resulting is a less pronounced solvatochromic shift and less intensity due to the small population in this orientation). In subsequent spectra showing two resonance features, we apply these assignments to describe molecular rulers interacting with the silica substrate either through the −OH ("NO_2 up") as in pNP or through the chromophore $-NO_2$ ("NO_2 down") as in pNAs (Figure 4).

We note that polarization-dependent measurements of SH intensity proved inconclusive in confirming these assignments. pNP has three nonzero $\chi^{(2)}$ elements.[60,61] Measuring the polarization-dependent SH intensity at a given wavelength enables one to determine these elements and, in principle, solute orientation in the laboratory frame of reference.[25,57,62] We carried

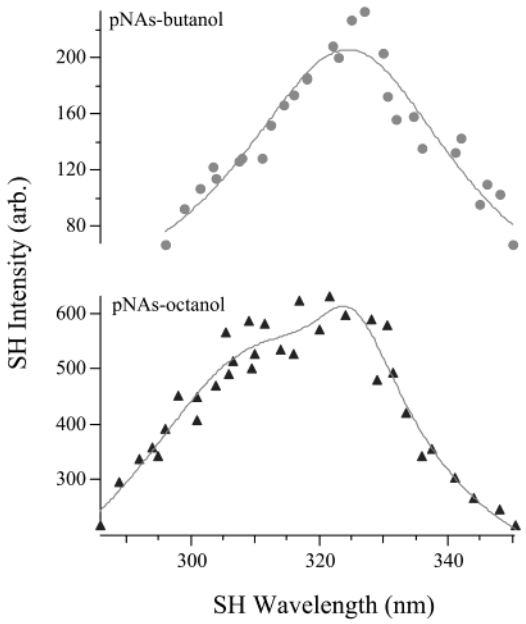

Figure 5. SH spectra of pNAs adsorbed to a hydrophilic/butanol interface (upper panel) and hydrophilic/octanol interface (lower panel). Solute concentrations in both samples were 1.4 mM. Solid lines represent fits to the experimental data according to eqs 2−5. Fit parameters appear in Table 2.

out polarization-dependent SH experiments for pNP at SH wavelengths of 296 nm (on the short wavelength side of the nonpolar feature) and 325 nm (on the long wavelength side of the polar feature). From these measurements, we calculated that the long axis of pNP is deflected $\sim 50 \pm 5°$ away from the surface normal at both wavelengths. The calculated orientation is only an ensemble average and does not unambiguously identify absolute orientation. For example, polarization-dependent measurements may lead to a calculated tilt angle of 40°, but data cannot distinguish an orientation of 40° ("up") from 140° ("down"). Only by measuring the phase of the SH signal relative to a known reference can absolute molecular orientations be determined. Such experiments are common at air/liquid and air/solid interfaces but prohibitively difficult at buried interfaces due to the dispersive nature of both phases.[63] We also note that the calculated molecular orientations are slightly larger than the SH "magic angle" of 39° described by Simpson and Rowlen.[64] This difference suggests that, whatever contribution surface roughness may make to SH intensity measurements, the solutes preferentially adopt an "in-plane" arrangement when adsorbed to the weakly associating hydrophilic/cyclohexane solid/liquid interface.

3B. pNAs at Strongly Associating Interfaces. Figure 5 shows SH spectra of pNAs adsorbed to hydrophilic/1-butanol and hydrophilic/1-octanol solid/liquid interfaces. When comparing these spectra, it is important to realize that the systems are identical except for solvent identity: the surfaces are the same, the solutes are the same, and the concentrations in bulk solution are the same. Fitting the butanol spectrum to two features leads to a major band at 321 nm and a smaller band at 303 nm. On the basis of the preceding analysis of the silica/cyclohexane data, we assign the long wavelength feature to a "NO_2 down" orientation in which the polar end of the pNAs solute interacts with the hydrophilic substrate. The 303 nm feature in the butanol spectrum corresponds to a less polar, "NO_2 up" orientation. The short wavelength feature has a transition wavelength very similar to that of pNAs in bulk butanol. Similar behavior is observed for pNAs adsorbed to the hydrophilic/1-octanol solid/liquid

interface. The long wavelength band is centered at 324 nm while the short wavelength feature appears at 307 nm.

Two differences between the butanol and octanol SH spectra are worth noting. First, both features in the octanol system appear at a (slightly) *longer wavelength* than in the butanol spectrum, despite the fact that pNAs has an identical bulk solution excitation wavelength (303 nm) in both solvents. Furthermore, bulk 1-butanol has a static dielectric constant ($\epsilon = 17$) that is twice that of 1-octanol ($\epsilon = 8.5$), meaning that one might expect the 1-octanol interface to form a *less* polar interfacial region than 1-butanol.

Second, the intensity distributions between the short and long wavelength features in the two spectra are reversed. In the butanol spectrum, the long wavelength feature carries more than 3 times the integrated intensity found in the short wavelength feature (e.g., $|A_b|^2 > 3|A_a|^2$). In contrast, the octanol spectrum features a very prominent short wavelength feature that is 7 times stronger than the long wavelength feature. Given the similarities between the two systems—same surfaces, same solutes (and similar bulk concentrations), and equivalent solvent−substrate interactions—we attribute these differences to relative populations of solutes in the $-NO_2$ up and $-NO_2$ down orientations. At the hydrophilic/butanol interface, more solutes interact with the substrate through the $-NO_2$ group, whereas this mechanism is inhibited at the hydrophilic/octanol interface. These results are consistent with earlier studies of solvent polarity at strongly associating interfaces that found regions of significantly reduced polarity at boundaries between silanol terminated silica and long chain alcohol solvents.[12]

3C. Molecular Rulers at Strongly Associating Interfaces. When comparing spectra from the hydrophilic/butanol and hydrophilic/octanol solid/liquid systems, speculation is limited by uncertainty about the interface itself. SHG experiments sample the anisotropic, interfacial region, but data contain no information about how far from the surface this region extends. Experiments cannot distinguish—a priori—chromophores adsorbed directly to the solid substrate from solutes under the influence of surface-induced polar ordering in the adjacent solvent layer. Profiling interfacial polarity across strongly associating interfaces requires systematically varying the equilibrium distribution of solvent sensitive chromophores relative to the hydrophilic solid surface. The alcohol surfactants described in section 2B can accomplish this goal.

Figures 6 and 7 show SH spectra of C_2 (Figure 6) and C_5 (Figure 7) molecular rulers adsorbed to hydrophilic/butanol and hydrophilic/octanol solid/liquid interfaces. The C_2 and C_5-octanol spectra were fit with two features as described above (eq 5). Optimized wavelengths and line strength terms appear in Table 2. Repeated attempts to fit the C_2 and C_5-butanol data with two features led to large disparities in line strengths (A_a and A_b in eqs 4 and 5) and large uncertainties in band positions. Consequently, spectra from C_2 and C_5-butanol systems were fit using a single resonance component (eq 3).

The C_2-butanol and C_2-octanol spectra in Figure 6 differ significantly from each other. The single resonance feature in the 1-butanol spectrum is centered at 316 nm. The C_2-octanol spectrum shows a band at the same wavelength (316 nm), but a second feature with significant intensity appears at a much shorter wavelength (296 nm). Two features in the C_2-octanol spectrum imply that 1-octanol creates two distinct environments at the solid/liquid interface, whereas the 1-butanol/hydrophilic interface is more homogeneous (and more polar) than bulk solution.

Again, solvatochromic considerations lead us to conclude that the hydrophilic/octanol solid/liquid interface contains a region

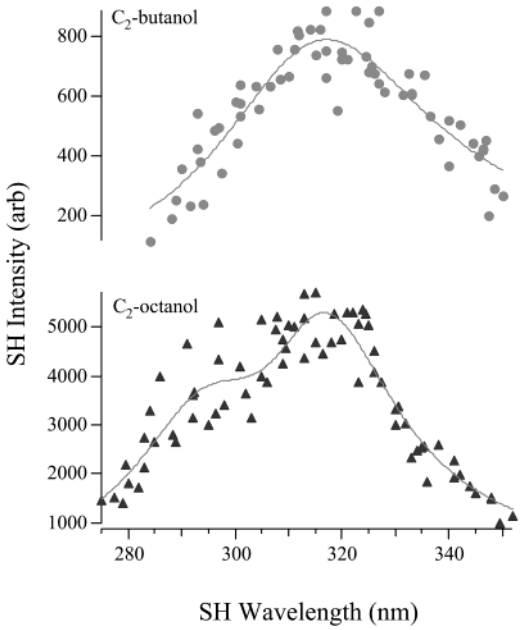

Figure 6. SH spectra of C_2 rulers adsorbed to a hydrophilic/butanol interface (upper panel) and hydrophilic/octanol interface(lower panel). Solute concentrations in both samples were 1.2 mM. Solid lines represent fits to the experimental data according to eqs 2−5. Fit parameters appear in Table 2.

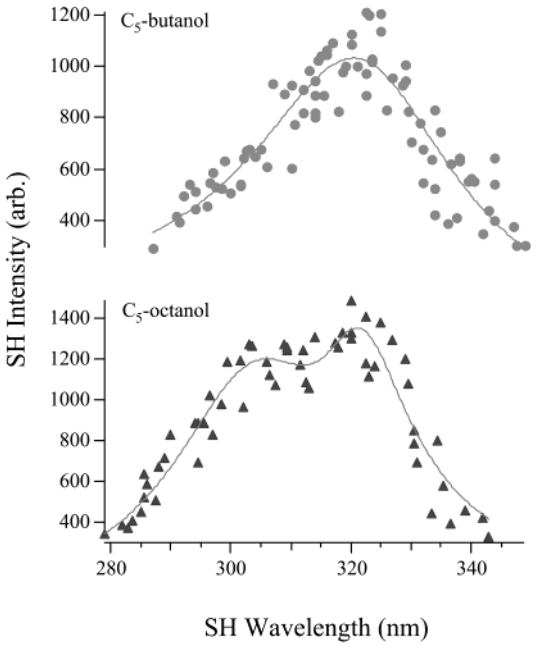

Figure 7. SH spectra of C_5 rulers adsorbed to a hydrophilic/butanol interface (upper panel) and hydrophilic/octanol interface(lower panel). Solute concentrations in both samples were 1.4 mM. Solid lines represent fits to the experimental data according to eqs 2−5. Fit parameters appear in Table 2.

that is much less polar than the hydrophilic/butanol boundary. Assigning the 296 nm feature in the C_2-octanol spectrum to an $-NO_2$ up orientation requires that the ruler chromophore samples a nonpolar environment similar to that experienced by the C_2 ruler in bulk alkanes. Furthermore, this nonpolar region can extend at least 1 nm away from the solid surface, where 1 nm corresponds to the separation between the chromophore $-NO_2$ group and the silica surface assuming that the C_2 ruler hydrogen bonds through its $-OH$ group and is oriented

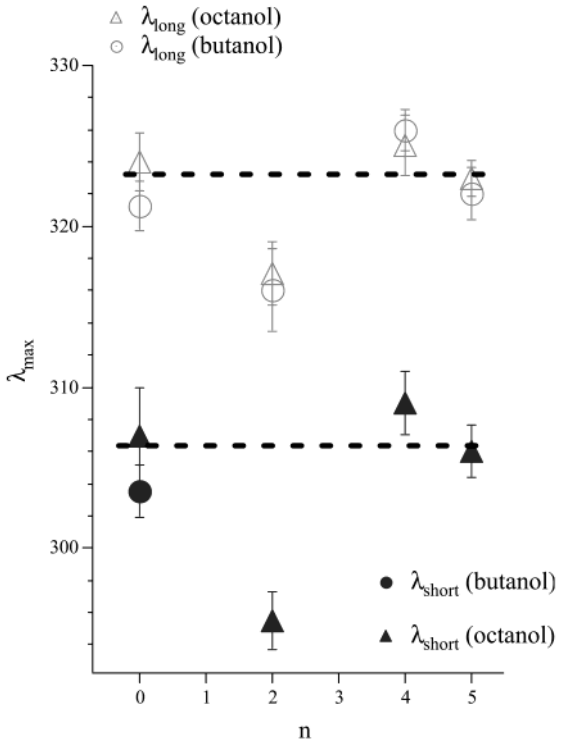

Figure 8. SH maxima plotted as a function of ruler length. Open symbols correspond to the long wavelength component obtained from fitting spectra shown in Figures 5−7. Filled symbols correspond to the short wavelength component of the same spectra. Triangles represent data from systems in which 1-octanol was the solvent, and circles are used for butanol solvent systems.

approximately normal to the silica substrate. The length of a fully extended 1-octanol molecule is ∼1.2 nm.

As with the C_2 data, significant differences exist between the C_5-butanol and C_5-octanol spectra. The C_5-butanol spectrum is fit to a single feature (324 nm). The C_5-octanol spectrum again shows two distinct bands with approximately equal intensity. Again, the two distinct features in the octanol spectrum suggest two regions of differing polarity at the hydrophilic/1-octanol solid/liquid interface. In contrast, the 1-butanol system appears to be more homogeneous. The short wavelength feature at 306 nm in the octanol system coincides with the absorbance maximum of the C_5 ruler in bulk octanol. Again, assuming hydrogen bonding through the ruler −OH and an approximately normal orientation relative to the hydrophilic substrate, the short wavelength feature limits the effective width of the nonpolar region to ∼1.4 nm, the separation between the nitro group of the ruler's hydrophobic chromophore and the −OH group.

The wavelength results from Table 2 are plotted in Figure 8 as a function of alkyl spacer chain length, *n*. C_0 corresponds to the bare chromophore, pNAs. Also included are results for the C_4 ruler adsorbed to both hydrophilic/1-butanol and hydrophilic/1-octanol interfaces. When pNAs is used to probe strongly associating solid/liquid systems, SH spectra show that butanol creates a (slightly) less polar interfacial environment than octanol despite having a higher dielectric constant. In both systems, the interface partitions into a polar and nonpolar region, with the latter being more pronounced in the hydrophilic/octanol system. This situation changes when the chromophore is allowed to move away from the surface and into the solvent. The hydrophilic/octanol system maintains two distinct regions of differing polarity even at distances probed by the longest molecular ruler, C_5. For both the C_4 and C_5 rulers, the less polar region exhibits static dielectric properties similar to that of bulk

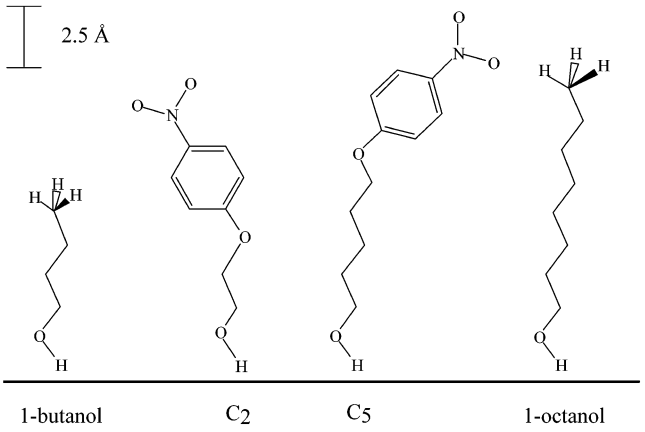

Figure 9. Molecular structures of C_2 and C_5 molecular rulers as well as 1-butanol and 1-octanol. Molecules are drawn to scale according to geometries predicted by GAMESS.

octanol as evidenced by very similar excitation wavelengths. However, data from hydrophilic/butanol systems suggest that the less polar region probed by pNAs vanishes very close to the polar solid substrate. For both the butanol and octanol systems, the C_2 ruler samples the least polar environment probed by any of the rulers; the single feature in the C_2-butanol spectrum is significantly blue-shifted from the other C_n-butanol spectra, and the C_2-octanol spectrum exhibits significant intensity in a feature centered at 296 nm, an excitation wavelength similar to that of pNAs in nonpolar solvents.

Simple geometric considerations can be used to understand these observations qualitatively. Figure 9 depicts structures of butanol, octanol, and the C_2 and C_5 rulers. The structures are shown in all-trans conformations and are drawn to scale. If both the butanol solvent and the C_2 ruler hydrogen bond to the surface through their respective −OH groups, then the ruler chromophore can extend beyond the first solvent layer and be less susceptible to surface-induced changes in the local solvation environment. Change the solvent to octanol, however, and the chromophore can be surrounded completely by alkyl chains. A fully extended octanol molecule spans 1.2 nm from −OH to the terminal methyl group. The length of a fully extended C_2 ruler is slightly less than 1 nm, meaning that the C_2 ruler chromophore can be completely enveloped in a nonpolar, alkane-like environment. Chromophores in this environment will not be able to interact with surface silanol groups or with solvent alcohol groups. We note that fully hydroxylated silica substrates have surface silanol concentrations of $4.8 \times 10^{14}/\text{cm}^2$ or ∼ 22 Å^2/OH group.[58,65] This concentration matches almost exactly surface concentrations of condensed-phase monolayers of all-trans alkyl chains,[5] meaning that the *n*-alcohol solvents can pack at the interface in a 1:1 ratio with surface silanol groups. Such close registry and extended interchain interactions may very well induce a solidlike phase in the first solvent layer similar to surface structures observed in X-ray scattering and NLO studies of long chain alcohols adsorbed to different liquid surfaces.[3,66,67]

A fully extended C_5 ruler spans 1.5 nm. Thus, an all-trans C_5 ruler will extend its chromophore beyond the first layer of octanol solvent. Earlier work suggested that long chain alcohol solvents may form bilayer structures at strongly associating interfaces.[10,12] Such structures would propagate the nonpolar region more than 2 nm away from the surface into bulk solution. SH results from molecular rulers do not support this picture. Once the ruler chromophore can extend beyond the first solvent layer, SH data show that ruler chromophores sample a local polarity similar to that of bulk octanol.

4. Conclusions

The intrinsic width of a solid/liquid interface can be defined in many ways depending on the property (density, refractive index, etc.) one chooses. Our interests lie in understanding how surfaces affect chemical solvation and identifying how far into solution surface effects extend. Using a series of new solvatochromic surfactants, we have begun to profile local polarity across strongly associating solid/liquid interfaces. The surfactants can function as molecular rulers: one end hydrogen bonds to a hydrophilic substrate, and the pNAs-based, hydrophobic chromophore probes solvent polarity at distances from the surface determined by the headgroup−chromophore separation. Local solvent polarity is determined by acquiring the resonance-enhanced second harmonic spectrum of the chromophores and comparing intensity maxima in the SH spectrum with excitation maxima in bulk solution. Results show that the bare pNAs chromophore samples two distinctly different environments at the weakly associating, hydrophilic/cyclohexane solid/liquid interface. Comparing intensity maxima with a similar spectrum from pNP adsorbed to the same interface leads us to conclude that the two different environments result from two different solute orientations. Molecular rulers enable us to localize solvent-sensitive chromophores at different distances from the hydrophilic, silica surface. We find that the hydrophilic/1-butanol interface presents a more polar environment than bulk butanol although the origin of this behavior remains uncertain. In contrast, the hydrophilic/1-octanol interface partitions into two distinct regions: one that is more polar than bulk and one that is less polar. The less polar region probed by the C_2 ruler exhibits local polarity similar to that of nonpolar, saturated hydrocarbons. When probed with C_4 and C_5 rulers, this less polar region exhibits solvent polarity similar to that of bulk 1-octanol, leading us to conclude that surface effects on solvent polarity extend no more than one solvent layer into solution for these strongly associating solid/liquid systems.

References and Notes

(1) Nigam, S.; deJuan, A.; Rutan, S. C. *Anal. Chem.* **1999**, *71*, 5225.
(2) Nigam, S.; Stephens, M.; deJuan, A.; Rutan, S. C. *Anal. Chem.* **2001**, *73*, 290.
(3) Sefler, G. A.; Du, Q.; Miranda, P. B.; Shen, Y. R. *Chem. Phys. Lett.* **1995**, *235*, 347.
(4) Safran, S. A. *Statistical Thermodynamics of Surfaces, Interfaces and Membranes*; Addison-Wesley Publishing Co.: New York, 1994.
(5) Adamson, A. W. *Physical Chemistry of Surfaces*, 5th ed.; John Wiley and Sons: New York, 1990.
(6) Benjamin, I. *J. Phys. Chem. A* **1998**, *102*, 9500.
(7) Lum, K.; Chandler, D.; Weeks, J. D. *J. Phys. Chem. B* **1999**, *103*, 4570.
(8) Makov, G.; Nitzan, A. *J. Phys. Chem.* **1994**, *98*, 3459.
(9) Pratt, L. R. *J. Phys. Chem.* **1992**, *96*, 25.
(10) Gang, O.; Wu, X. Z.; Ocko, B. M.; Sirota, E. B.; Deutsch, M. *Phys. Rev. E* **1998**, *58*, 6086.
(11) Zhang, X.; Cunningham, M. M.; Walker, R. A., submitted for publication.
(12) Zhang, X.; Walker, R. A. *Langmuir* **2001**, *17*, 4486.
(13) Shen, Y. R. *Nature (London)* **1989**, *337*, 519.
(14) Hansen, R. L.; Harris, J. M. *Anal. Chem.* **1998**, *70*, 2565.
(15) Piasecki, D. A.; Wirth, M. J. *Langmuir* **1994**, *10*, 1913.
(16) Dong, Y.; Xu, Z. *Langmuir* **1999**, *15*, 4590.
(17) Gruzdkov, Y. A.; Parmon, V. N. *J. Chem. Soc., Faraday Trans.* **1993**, *89*, 4017.
(18) He, G.; Xu, Z. *J. Phys. Chem. B* **1997**, *101*, 2101.
(19) Higgins, D. A.; Byerly, S. K.; Abrams, M. B.; Corn, R. M. *J. Phys. Chem.* **1991**, *95*, 6984.
(20) Miranda, P. B.; Pflumio, V.; Saijo, H.; Shen, Y. R. *Chem. Phys. Lett.* **1997**, *264*, 387.
(21) Salafsky, J. S. *Chem. Phys. Lett.* **2001**, *342*, 485.
(22) Saroja, G.; Samanta, A. *Chem. Phys. Lett.* **1995**, *246*, 506.
(23) Shang, X.; Benderskii, A. V.; Eisenthal, K. B. *J. Phys. Chem. B* **2001**, *105*, 11578.
(24) Zhang, X.; Esenturk, O.; Walker, R. A. *J. Am. Chem. Soc.* **2001**, *123*, 10768.
(25) Tamburello-Luca, A. A.; Hebert, P.; Brevet, P. F.; Girault, H. H. *J. Chem. Soc., Faraday Trans.* **1996**, *92*, 3079.
(26) Tamburello-Luca, A. A.; Hebert, P.; Antoine, R.; Brevet, P. F.; Girault, H. H. *Langmuir* **1997**, *13*, 4428.
(27) Wang, H.; Harris, J. *J. Phys. Chem.* **1995**, *99*, 16999.
(28) Wang, H.; Callahan, P. M. *J. Chromatogr. A* **1998**, *828*, 121.
(29) Wang, H.; Borguet, E.; Eisenthal, K. B. *J. Phys. Chem. B* **1998**, *102*, 4927.
(30) Wirth, M. J.; Ludes, M. D.; Swinton, D. J. *Anal. Chem.* **1999**, *71*, 3911.
(31) Xu, Z.; Li, J.; Dong, Y. *Langmuir* **1998**, *14*, 1183.
(32) Yanagimachi, M.; Tamai, N.; Masuhara, H. *Chem. Phys. Lett.* **1992**, *200*, 469.
(33) Ishizaka, S.; Habuchi, S.; Kim, H. B.; Kitamura, N. *Anal. Chem.* **1999**, *71*, 3382.
(34) Burbage, J. D.; Wirth, M. J. *J. Phys. Chem.* **1992**, *96*, 5943.
(35) Castro, M. A.; Clarke, S. M.; Inaba, A.; Thomas, R. K. *J. Phys. Chem. B* **1997**, *101*, 8878.
(36) Lee, L. T.; Langevin, D.; Farnoux, B. *Phys. Rev. Lett.* **1991**, *67*, 2678.
(37) Messe, L.; Clarke, S. M.; Arnold, T.; Dong, C.; Thomas, R. K.; Inaba, A. *Langmuir* **2002**, *18*, 4010.
(38) Mitrinovic, D. M.; Zhang, Z.; Williams, S. M.; Huang, Z.; Schlossman, M. L. *J. Phys. Chem. B* **1999**, *103*, 1779.
(39) Mitrinovic, D. M.; Tikhonov, A. M.; Li, M.; Huang, Z.; Schlossman, M. L. *Phys. Rev. Lett.* **2000**, *85*, 582.
(40) Penfold, J.; Richardson, R. M.; Zarbakhsh, A.; Webster, J. R. P.; Bucknall, D. G.; Rennie, A. *J. Chem. Soc., Faraday Trans.* **1997**, *93*, 3899.
(41) Dang, L. X. *J. Phys. Chem. B* **2001**, *105*, 804.
(42) Fukunishi, Y.; Tateishi, T.; Suzuki, M. *J. Colloid Interface Sci.* **1996**, *180*, 188.
(43) Lee, S. H.; Rossky, P. J. *J. Chem. Phys.* **1994**, *100*, 3334.
(44) Michael, D.; Benjamin, I. *J. Chem. Phys.* **2001**, *114*, 2817.
(45) Senapati, S.; Chandra, A. *Chem. Phys.* **1999**, *242*, 353.
(46) Pohorille, A.; Wilson, M. A. *J. Chem. Phys.* **1996**, *104*, 3760.
(47) Schweighofer, K.; Benjamin, I. *J. Phys. Chem. A* **1999**, *103*, 10274.
(48) Senapati, S.; Berkowitz, M. L. *Phys. Rev. Lett.* **2001**, *87*, 6101.
(49) Michael, D.; Benjamin, I. *J. Phys. Chem.* **1995**, *99*, 16810.
(50) Steel, W. H.; Damkaci, F.; Nolan, R.; Walker, R. A. *J. Am. Chem. Soc.* **2002**, *124*, 4824.
(51) Suppan, P. *J. Photochem. Photobiol. A* **1990**, *50*, 293.
(52) Suppan, P.; Ghoneim, N. *Solvatochromism*; Royal Society of Chemistry: Cambridge, UK, 1997.
(53) Laurence, C.; Nicolet, P.; Delati, M. T.; Abboud, J. M.; Notario, R. *J. Phys. Chem.* **1994**, *98*, 5807.
(54) Matyushov, D. V.; Schmid, R.; Ladanyi, B. M. *J. Phys. Chem. B* **1997**, *101*, 1035.
(55) Corn, R. M.; Higgins, D. A. *Chem. Rev.* **1994**, *94*, 107.
(56) Shen, Y. R. *The Principles of Nonlinear Optics*; John Wiley and Sons: New York, 1984.
(57) Dick, B.; Gierulski, A.; Marowsky, G.; Reider, G. A. *Appl. Phys. B* **1985**, *38*, 107.
(58) Gee, M. L.; Healy, T. W.; White, L. R. *J. Colloid Interface Sci.* **1990**, *140*, 450.
(59) *CRC Handbook of Chemistry and Physics*, 72nd ed.; CRC Press: Boston, 1991.
(60) Bell, A. J.; Frey, J. G.; Vandernoot, T. J. *J. Chem. Soc., Faraday Trans.* **1992**, *88*, 2027.
(61) Higgins, D. A.; Abrams, M. A.; Byerly, S. K.; Corn, R. M. *Langmuir* **1992**, *8*, 1994.
(62) Zhuang, X.; Miranda, P. B.; Kim, D.; Shen, Y. R. *Phys. Rev. B* **1999**, *59*, 12632.
(63) Stolle, R.; Marowsky, G.; Schwarzberg, E.; Berkovic, G. *Appl. Phys. B* **1996**, *63*, 491.
(64) Simpson, G. J.; Rowlen, K. L. *Chem. Phys. Lett.* **2000**, *317*, 276.
(65) Iler, R. K. *The Chemistry of Silica*; Wiley-Interscience Publishers: New York, 1979.
(66) Morishige, K.; Kato, T. *J. Chem. Phys.* **1999**, *111*, 7095.
(67) Stanners, C. D.; Du, Q.; Chin, R. P.; Cremer, P.; Somojai, G. A.; Shen, Y. R. *Chem. Phys. Lett.* **1995**, *232*, 407.